Role of calcium in the regulation of mechanical power in insect flight

Shefa Gordon[†] and Michael H. Dickinson[‡§]

[†]Division of Neurobiology, Department of Molecular and Cell Biology, University of California, Berkeley, CA 94720; and [‡]Bioengineering Option, California Institute of Technology, Pasadena, CA 91125

Edited by David L. Denlinger, Ohio State University, Columbus, OH, and approved January 17, 2006 (received for review November 21, 2005)

Most flying insect species use ''asynchronous'' indirect flight muscles (A-IFMs) that are specialized to generate high mechanical power at fast contraction frequencies. Unlike individual contractions of ''synchronous'' muscles, those of A-IFMs are not activated and deactivated in concert with neurogenically controlled cycling of myoplasmic [Ca^{2+}] but rather are driven myogenically by oscillatory changes in length. The motor neurons of the A-IFMs, which fire at a rate much slower than contraction frequency, are thought to play the limited role of maintaining myoplasmic [Ca^{2+}] above the critical threshold that maintains the muscle in a stretch-activatable state. Despite this asynchronous form of excitation–contraction coupling, animals can actively regulate power output as required for different flight behaviors, although the neurobiological and biophysical basis of this regulation is unknown. While presenting tethered flying fruit flies, *Drosophila melanogaster*, with visual stimuli, we recorded membrane potential spikes in identified A-IFM fibers. We show that mechanical power output rises and falls in concert with the firing frequency of all A-IFM fibers and cannot be explained by differential recruitment of separately innervated motor units. To explore the hypothesis that myoplasmic [Ca^{2+}] might similarly rise and fall in concert with firing frequency, we genetically engineered *Drosophila* to express the FRET-based Ca^{2+} indicator cameleon selectively within A-IFMs. The results show that Ca^{2+} levels increase in proportion to muscle firing rate, both during spontaneous flight and when muscle spikes are elicited electrically. Collectively, these experiments on intact animals support an active role for [Ca^{2+}] in regulating power output of stretch-activated A-IFM.

cameleon | *Drosophila* | FRET | stretch activation

The remarkable proliferation and evolutionary success of flying insects is due in large part to the unique properties of the muscles that power their wings. Members of the most successful groups of insects, including the Dipteran order to which *Drosophila* belongs, possess mechanically activated asynchronous indirect flight muscles (A-IFMs) that oscillate at high frequency without cycle-by-cycle motor neuron activation (1, 2). A-IFMs have served as a useful model system for studies of muscle structure and function, particularly after the application of molecular and genetic approaches (3). The use of stretch activation and shortening deactivation at a constant level of activating Ca^{2+} liberates A-IFMs from the need for an extensive sarcoplasmic reticulum, thus permitting a greater percentage of internal volume to be dedicated to contractile fibrils and mitochondria (4). The motor neurons of the A-IFMs fire at a rate (≈5 Hz in *Drosophila*) well below contraction frequency (≈200 Hz in *Drosophila*), and Ca^{2+} is thought to be relegated to a permissive role of maintaining the muscle fibers in a stretch-activatable state (5).

In addition to simply generating sufficient power for sustained flight, another critical requirement of flight muscle is that its power output can be regulated as required for different flight maneuvers such as takeoffs, vertical ascents, and forward acceleration (6). Because oscillatory contraction rhythm is decoupled from neural drive, it is not clear how this active regulation is achieved. One possibility is that the role of Ca^{2+} is graded rather than binary, such that the nervous system adjusts the tonic level of Ca^{2+} through changes in the firing frequency of A-IFM motor neurons. In this study, we attempted to test this hypothesis in intact flying animals by genetically engineering flies to express a calcium indicator molecule in the A-IFMs. The results show the A-IFM spike rate, mechanical power, and intracellular calcium covary during flight in a way that is consistent with a power-regulating role of Ca^{2+}.

Results

To investigate the possibility that the power output of the flight motor is correlated with the firing rate in A-IFMs, we tethered wild-type fruit flies in front of a high-speed display monitor and recorded the membrane potential of identified muscle fibers using intracellular electrodes (Fig. 1 *a* and *b*). Each muscle ''spike'' represents a large excitatory junction potential in response to an action potential in the fiber's motor neuron. Vertical oscillation of a pattern of horizontal stripes at 0.08 Hz elicited a rhythmic regulation of power output as flies increase thrust and lift in response to rising stripes and decrease thrust and lift in response to falling stripes. An ≈2-fold change in power accompanied a 3-fold change in steady-state spike frequency (Fig. 1*c*). Such experiments were repeated for five different dorsal longitudinal muscle (DLM) fibers (cells 2–6) and all three dorsoventral muscle (DVM) fiber groups for a total of 111 separate experiments. We recorded a significant positive correlation in all cases (r ranged from 0.34 to 0.67; Table 1, which is published as supporting information on the PNAS web site). These results confirm that A-IFM spike frequency does vary during flight (7) and is positively correlated with mechanical power (8).

One possible means by which the fly's nervous system could regulate power is through differential recruitment of the 13 individual muscle cells within each bilateral DLM and DVM pair. To test this hypothesis, we performed a set of 14 separate pairwise recordings between synergist (DLM vs. DLM; DVM vs. DVM) and antagonist (DVM vs. DLM) fibers (Table 2, which is published as supporting information on the PNAS web site). In all cases the correlation in instantaneous spike frequency was very high (range 0.55–0.91) and significant. The results were consistent with prior studies suggesting that the A-IFM fibers are driven by a set of four loosely coupled central pattern generators, two that drive the five motor units of the DLMs and two that drive three motor units of the DVMs (9). We found no evidence for differential recruitment of fibers within each synergist pool. Thus, although changes in firing frequency might explain active modulation of power, changes in recruitment cannot.

Conflict of interest statement: No conflicts declared.

This paper was submitted directly (Track II) to the PNAS office.

Abbreviations: A-IFM, asynchronous indirect flight muscle; DLM, dorsal longitudinal muscle; DVM, dorsoventral muscle; CFP, cyan fluorescent protein; YFP, yellow fluorescent protein.

[§]To whom correspondence should be addressed. E-mail: flyman@caltech.edu.

© 2006 by The National Academy of Sciences of the USA

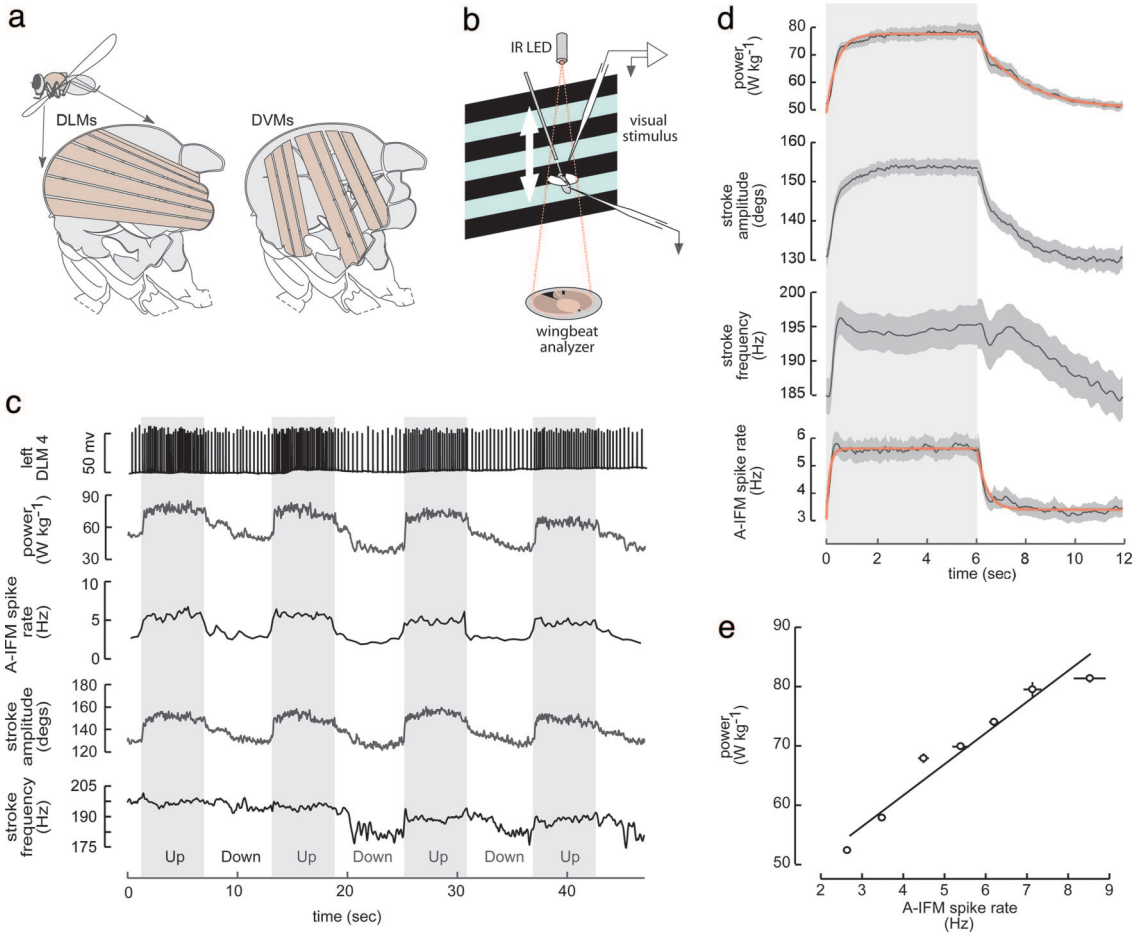

Fig. 1. Mechanical power covaries with A-IFM firing rate. (*a* and *b*) Muscle fibers were recorded during flight in tethered flies. Changes in flight behavior were elicited visually by using a visual grating pattern that drifted alternately up and down. Stroke frequency and amplitude were measured with an optical sensor. (*c*) Flies increased and decreased stroke amplitude and stroke frequency to effect changes in mechanical power in response to the upward and downward motion of the visual stimulus. Power modulations correlated with changes in muscle firing rates. (*d*) In flight segments selected for rapid changes in A-IFM firing rate, the time course of mechanical power rises much more rapidly than it falls (mean ± SEM, dark shading). Red lines indicate first-order exponential fits through the data. The up stimulus is indicated by light gray background shading ($n = 30$). The down stimulus has no background shading ($n = 22$). (e) Steady-state power plotted versus steady-state A-IFM rate. Sixty-two flight sequences were averaged over a 4-s window (Fig. 3*b* shows seconds 2–6 after the onset of the up stimulus). Data were binned by mean A-IFM firing rate; error bars represent SEM.

To examine the time course of changes in power output, we selected from our data set examples in which the changes in spike frequency elicited by the vertically oscillating visual patterns were rapid enough to approximate a step response (Fig. 1*d*). The results indicate that power rises rapidly after a step increase in spike rate but decays slowly after a step decrease in spike rate. The time constants for the rise and fall in power were 0.442 and 1.79 s, respectively, compared with time constant values of 0.134 and 0.329 s for the corresponding changes in spike rate. These results indicate that, if spike rate is responsible for modulating power, it must act by means of an intracellular intermediate that permits rapid activation but exhibits slow deactivation (Fig. 3*a*, which is published as supporting information on the PNAS web site).

Further evidence for a slow decay in muscle power is seen in the complex relationship between stroke frequency and stroke amplitude after a step decrease in spike rate. Immediately after spike rate drops, stroke amplitude rapidly decays whereas stroke frequency transiently rises before eventually slowly decreasing (Fig. 1*d*). Prior studies suggest that periods of anticorrelation between stroke amplitude and stroke frequency are due to the activity of the tiny twitch-type steering muscles, which can elicit rapid changes in stroke amplitude (10, 11). Because mechanical power is roughly proportional to the cubed product of stroke frequency and stroke amplitude (see *Methods* and ref. 6), a decrease in stroke amplitude must result in an increase in stroke frequency as long as the power input to the mechanical system is constant. This is a likely explanation for the peculiar rise in stroke frequency when the visual pattern starts to move downward. After the control muscles elicit a rapid drop in stroke amplitude, the oscillatory system responds with an increase in stroke frequency, which then decays as the total mechanical power provided by the A-IFMs slowly falls.

One possible explanation for the long time course in the decay of mechanical power after rapid drops in spike rate is that the activation of cross-bridges within the A-IFMs is regulated by cytoplasmic [Ca^{2+}] (8). Although Ca^{2+} is thought to play a permissive role in stretch activation, we suggest that it plays a regulatory role, albeit not on a contraction-by-contraction basis. According to this hypothesis, when elevated power is required, spike rate rises to drive additional Ca^{2+} into the cell via voltage- and glutamate-gated channels, thereby recruiting cross-bridges or entire fibrils deep within the giant muscle cells. The minute amount of sarcoplasmic reticulum, which is characteristic of A-IFMs, would explain why it may take several seconds for power levels to drop after a decrease in spike rate (Figs. 1*d* and

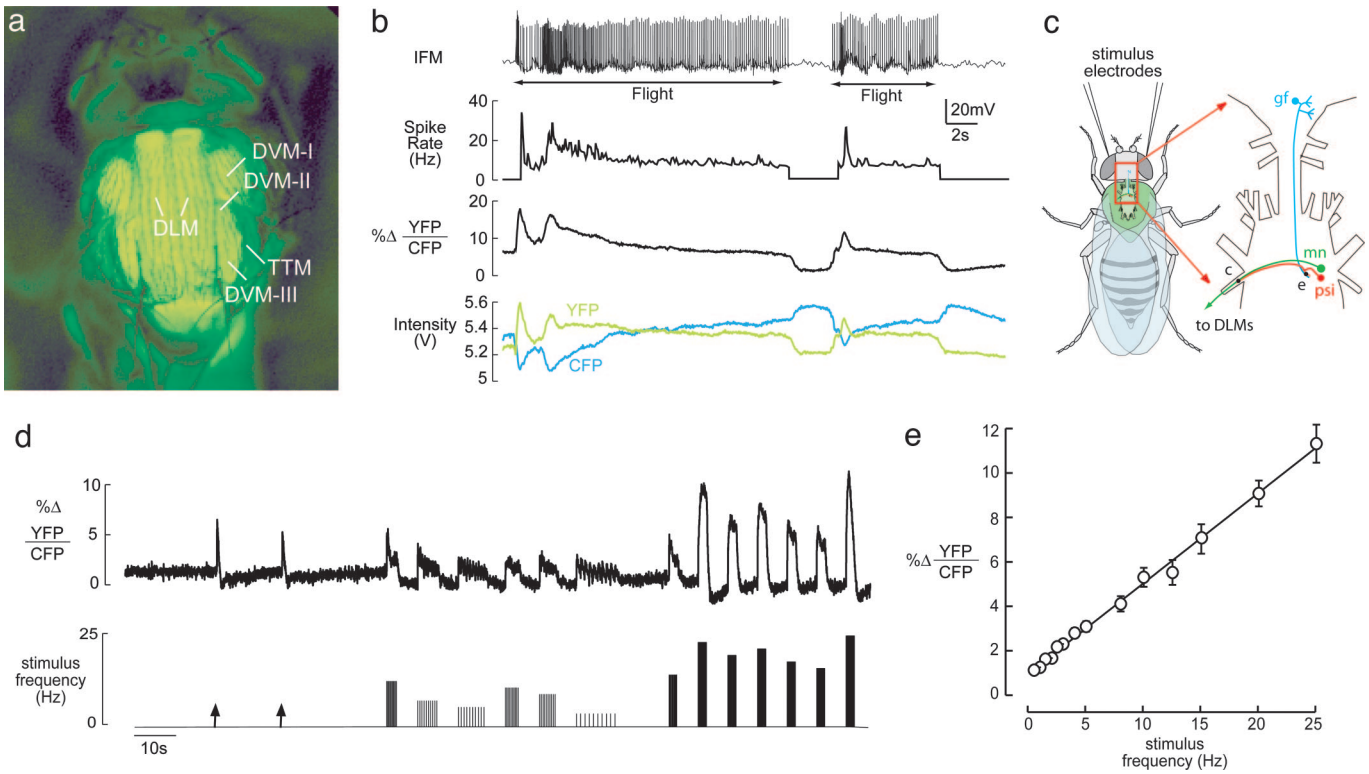

Fig. 2. Intracellular calcium correlates with muscle activity. (*a*) Cameleon 3.1 expressed specifically in A-IFM (both DLMs and DVMs) but not synchronous muscle (e.g., tergotrochanteral muscle, TTM). (*b*) During flight, increased FRET from YFP to CFP indicated that calcium levels varied with A-IFM spike rate. (*c*) Current injected in the brain evoked simultaneous activity in A-IFMs by means of the giant fiber (gf) system. mn, motorneuron; psi, peripherally synapsing interneuron; e, electrical synapse; c, chemical synapse. (*d*) In the absence of flight, calcium responses to single pulses (arrows) and trains of electrical stimulation at 4, 2, 1.5, 3, 2.5, 1, 5, 20, 12.5, 15, 10, 8, and 25 Hz. Bar height is only qualitatively proportional to stimulus frequency. (*e*) Steady-state calcium levels in response to brain stimulation (mean of stimulus pulses 2–10 in each train) plotted versus stimulus frequency.

3*a*). Whereas power recruitment may depend on the rapid entry of Ca^{2+} down its electrochemical potential, relaxation requires actively pumping Ca^{2+} across a membrane. To explore this hypothesis, we created lines of transgenic flies that expressed the FRET-based Ca^{2+} indicator molecule cameleon (12, 13) under the control of the promoter for Act88F, a structural gene that is unique to the A-IFMs (14). One of the 10 stable lines that we generated (an insert on the third chromosome) displayed bright fluorescence that was restricted to the A-IFMs (Fig. 2*a*). To measure *in vivo* changes in FRET, we tethered the flies within the light path of a dual-emission fluorescent microscope equipped with two independent photomultiplier detectors that measured the emissions at 485 nm [cyan fluorescent protein (CFP)] and 535 nm [yellow fluorescent protein (YFP)] (Fig. 4, which is published as supporting information on the PNAS web site). As indicated in Fig. 2*b*, the system was sensitive enough to detect changes attributed to increases in intracellular $[Ca^{2+}]$ during flight. The strong correlation between spike rate and FRET is apparent. In all cases, the onset of flight was accompanied by a brief burst in A-IFM spike rate and a concomitant rise in FRET. Additional increases in A-IFM spike rate within flight bouts were correlated with further increases in the ratio of YFP/CFP emission. Although early versions of cameleon exhibited sensitivity to acid conditions, control experiments showed that the changes in FRET were not caused by activity-dependent changes in pH (Fig. 5, which is published as supporting information on the PNAS web site).

When flying within the beam of the fluorescent microscope, the flies were not particularly sensitive to a moving visual display, presumably because the intense excitation interfered with their visual sensitivity. For this reason, we were not able to elicit active modulation of flight behavior to perform an extensive correlational analysis of FRET and spike rate. Furthermore, because the muscle cells are large, it is not possible to pass enough current to depolarize the cells directly. For this reason, we chose a different preparation for accurately quantifying the relationship between A-IFM spike rate and Ca^{2+}-based FRET. The strong and well characterized synaptic connections in the giant fiber escape pathway provide a convenient way of activating the DLMs at arbitrary frequencies in intact flies (15, 16). Short shocks delivered by bipolar electrodes placed in the visual lobes of the brain are sufficient to elicit one-for-one junction potentials simultaneously in the all DLMs via a short-latency bisynaptic pathway (Figs. 2*c* and 5*b*). With this arrangement, we were able to drive the DLMs across the excitation frequency range that they experience in flight while measuring the changes in Ca^{2+}-based FRET (Fig. 2*d*). The results show that steady-state FRET levels are linearly proportional to the frequency of DLM excitation (Fig. 2*e*). During steady-state flight, a 3-fold increase in spike frequency (from 3 to 9 Hz) results in a 1.7-fold increase in power output (Fig. 1*e*), which corresponds to an ≈2-fold change in %YFP/CFP emission (Fig. 2*e*). Sustained high stimulus frequencies (up to 25 Hz, at which point synapses in the pathway began to fail) elicited further increases in Ca^{2+}-based FRET. This finding suggests that $[Ca^{2+}]$ is not saturated at the endogenous activation frequencies measured in stable flight. Similar results were obtained in experiments by using fluorescent indicators injected into single fibers to measure $[Ca^{2+}]$ (Fig. 6, which is published as supporting information on the PNAS web site).

Discussion

The results of this study support the hypothesis that cytoplasmic Ca^{2+} plays an active role in regulating the mechanical power output of the stretch-activated, asynchronous IFMs of insects. The conclusions are based on two separate observations in intact animals: (*i*) that A-IFM spike rate during flight is proportional to power output, and (*ii*) that intracellular free Ca^{2+} is proportional to spike rate. These experiments, which were designed to explore muscle biophysics in intact animals, are limited in two ways. First, we have not demonstrated that a direct experimental manipulation of intracellular Ca^{2+} elicits an elevation in power output. Although theoretically possible using caged compounds, this task is complicated by the fact that a change in net power output would require simultaneous activation of a sizeable fraction of the 26 individual giant muscle fibers. Second, we have not provided an absolute measure of $[Ca^{2+}]$ during flight. This latter point is most important, because amplitude of stretch-activated force in skinned A-IFM fibers rises from zero to saturation quite steeply against a small increase in $[Ca^{2+}]$ (17). For the Ca^{2+}-regulation hypothesis to be tenable, $[Ca^{2+}]$ in the A-IFM cells of flying flies must sit below the saturating levels of their intrinsic Ca^{2+}-activation curve; otherwise a spike-frequency mediated rise in $[Ca^{2+}]$ could not evoke any change in contraction mechanics. This test is thus constrained by the recent observations indicating that only a fraction of the $[Ca^{2+}]$ increase required to elicit full isometric contraction is required to elicit full stretch-mediated contraction (17) and that a large fraction of troponin C in A-IFMs may be a stretch-sensitive isoform with a narrow dependence on $[Ca^{2+}]$ (18). Thus, for rises in intracellular $[Ca^{2+}]$ to have an effect on cross-bridge recruitment and power output, the *in vivo* operating level during normal flight must be far to the left on the Ca^{2+} activation curve, or else the fly would have little mechanical power reserve. Future modifications of our experimental paradigm should permit measurements of absolute Ca^{2+} to test this clear prediction. These observations should also be of use in refining new biophysical models of stretch activation (17–19).

Methods

Tethered Flight. Female 1- to 5-day old *Drosophila melanogaster* were rigidly affixed at the anterior base of the notum to the end of a 0.1-mm-diameter stainless steel rod by using a light-activated adhesive as described (6). For fluorescence experiments, flies were tethered ventrally by first removing leg segments distal to the coxae and then gluing the sternum to a bent rod at a 30° angle to approximate natural body position during hovering. After recovery, tethered flies were maintained in a humidified chamber for 1–7 h before experimentation. To elicit visually mediated flight responses, we used a Picasso CRT Image Synthesizer (Innisfree) and oscilloscope monitor (Tektronix 608) to present a horizontal grating that drifted vertically according to a 12-s square wave, alternating every 6 s between upward drift (eliciting an increase in flight power) and downward drift (eliciting a reduction in flight power).

Calculation of Mechanical Power. Wingbeat amplitude and frequency were measured as previously described by optically tracking the shadow of the two wings cast from an IR beam aimed at a calibrated photovoltaic sensor (Fig. 1*b*) (20). Mass-specific mechanical power was estimated from flight kinematics and fly morphometrics as described (6, 21) but modified according to more accurate measurements of mean wing drag during tethered flight (22). Briefly, muscle mass-specific mechanical power, P^*_{mech}, was calculated by summing the estimates of mass specific profile power, P^*_{pro}, and induced power, P^*_{ind} (i.e., $P^*_{mech} = P^*_{pro} + P^*_{ind}$). This model assumes that there is sufficient elastic storage to ignore inertial power and that flight muscle accounts for 30% of total body mass (6). The expressions for P^*_{pro} and P^*_{ind}, given previously (6), simplify to $P^*_{pro} = C_{pro}\,\Phi^3 n^3$ and $P^*_{ind} = C_{ind}\,\Phi^{-1/2}$, where Φ is mean stroke amplitude, n is stroke frequency, and C_{pro} and C_{ind} are constants derived by combining all of the time-invariant morphometric terms in the power equations (23). In these experiments, we calculated the constants C_{pro} and C_{ind} to be 1.44×10^{-7} m^2 and 10.5 m^{2}s^{-3}, respectively.

Electrophysiology. Individual fibers were identified by using external landmarks (24) and recorded intracellularly (IR-283, Neurodata) with 10-MΩ glass microelectrodes filled with 150 mM KCl plugged with 1% agar to prevent leakage. Flies were grounded with an electrode in the abdomen. Data were acquired at 5 kHz (Digidata 1320a data acquisition board, Axon Instruments) and high-pass-filtered off-line at 50 Hz through a four-pole, zero-phase-delay digital Butterworth filter. Spike rate was calculated from the instantaneous interspike interval. All analyses were performed by using custom software written in MATLAB (Mathworks).

Stimulation of the giant fiber required two etched tungsten electrodes placed medially to the compound eyes with constant voltage supplied by a stimulus isolation unit (SIU-90, Neurodata). Giant fiber stimulus threshold was determined by increasing voltage levels of the 200-μs excitation pulse until a systemic twitch in the wings and abdomen was observed. In each experiment, the membrane potential recording was examined for synaptic potential failures after each stimulus artifact. Data were not included in the analysis if failure occurred two or more times in a train of 10 pulses or if spontaneous muscle spiking was observed.

Generation of Transgenic Flies. Cameleon 3.1 construct from R. Y. Tsien (University of California at San Diego, La Jolla) (13, 25) was subcloned into the NotI restriction site of a pW8 vector containing the Act88F promoter provided by J. Moore (Boston University, Boston) (14). P-element germ-line transformations of w^{1118} using standard techniques yielded stable lines of flies expressing cameleon specifically in the A-IFMs. Variant cameleon lines are described in *Supporting Text*, which is published as supporting information on the PNAS web site.

Fluorescence Microscopy. The specimen stage of a Nikon Optiphot-2 microscope was removed and replaced with a micromanipulator fitted with an adapter for the fly tether. Illumination from a Mercury arc lamp (Hg 100 W; Episcopic-Fluorescence Attachment EF-D, Nikon) passed through neutral-density filters to prevent the fly from overheating. For each application, standard filter cubes (Chroma Technology) controlled transmittance to the specimen. Dual-emission ratio imaging of cameleon (Fig. 4) used a 440DF30 excitation filter to excite the donor fluorophore, CFP. Incident light was reflected to the specimen with a dichroic mirror (455DRLP); emitted fluorescent light was divided with a beamsplitter mirror (515DCLP) and filtered for CFP emission (480DF30) and for YFP emission (535DF25). The fluorescence signal from the entire thorax was measured with two photomultiplier tubes (Model 814, Photon Technology International) in analogue mode (τ = 5 ms). Data were filtered off-line with a 12.5 Hz low-pass Butterworth.

We thank Mark Tanouye and Udi Isacoff for helpful discussions and support in creating transgenic flies. We acknowledge Mark Frye for help with electrophysiology and Gerry Rubin for help generating Fig. 2*a* and assistance with embryo injection of DNA constructs. S.G. was supported in part by National Institutes of Health National Research Service Award Trainee Appointment T32 GM07048. The project was funded through the support of the Packard Foundation and the National Science Foundation (IBN-9723424).

1. Boettiger, E. G. & Furshpan, E. (1952) *Biol. Bull.* **102,** 200–211.
2. Pringle, J. W. S. (1949) *J. Physiol.* **108,** 226–232.
3. Vigoreaux, J. (2005) *Nature's Versatile Engine: Insect Flight Muscle Inside and Out* (Springer, New York), p. 310.
4. Josephson, R. K., Malamud, J. G. & Stokes, D. R. (2000) *J. Exp. Biol.* **203,** 2713–2722.
5. Machin, K. E. & Pringle, J. W. S. (1960) *Proc. R. Soc. London Ser. B* **152,** 311–330.
6. Lehmann, F. O. & Dickinson, M. H. (1997) *J. Exp. Biol.* **200,** 1133–1143.
7. Smyth, T. & Yurkiewicz, W. J. (1966) *Comp. Biochem. Physiol. A Physiol.* **17,** 1175–1180.
8. Dickinson, M. H., Lehmann, F. O. & Chan, W. P. (1998) *Am. Zool.* **38,** 718–728.
9. Harcombe, E. S. & Wyman, R. J. (1978) *J. Comp. Physiol. A* **123,** 271–279.
10. Heide, G. & Götz, K. G. (1996) *J. Exp. Biol.* **199,** 1711–1726.
11. Dickinson, M. H. & Tu, M. S. (1997) *Comp. Biochem. Physiol. A Physiol.* **116,** 223–238.
12. Petrou, S., Bowser, D. N., Nicholls, R. A., Panchal, R. G., Smart, M. L., Reilly, A. M. & Williams, D. A. (2000) *Clin. Exp. Pharmacol. Physiol.* **27,** 738–744.
13. Miyawaki, A., Llopis, J., Heim, R., McCaffery, J. M., Adams, J. A., Ikura, M. & Tsien, R. Y. (1997) *Nature* **388,** 882–887.
14. Barthmaier, P. & Fyrberg, E. (1995) *Dev. Biol.* **169,** 770–774.
15. Thomas, J. B. & Wyman, R. J. (1984) *J. Neurosci.* **4,** 530–538.
16. Wyman, R. J., Thomas, J. B., Salkoff, L. & King, D. G. (1984) in *Neural Mechanisms of Startle Behavior*, ed. Eaton, R. (Plenum, New York), pp. 133–160.
17. Linari, M., Reedy, M. K., Reedy, M. C., Lombardi, V. & Piazzesi, G. (2004) *Biophys. J.* **87,** 1101–1111.
18. Agianian, B., Krzic, U., Qiu, F., Linke, W. A., Leonard, K. & Bullard, B. (2004) *EMBO J.* **23,** 772–779.
19. Dickinson, M., Farman, G., Frye, M., Bekyarova, T., Gore, D., Maughan, D. & Irving, T. (2005) *Nature* **433,** 330–333.
20. Götz, K. G. (1987) *J. Exp. Biol.* **128,** 35–46.
21. Ellington, C. P. (1984) *Philos. Trans. R. Soc. London B* **305,** 145–181.
22. Fry, S. N., Sayaman, R. & Dickinson, M. H. (2005) *J. Exp. Biol.* **208,** 2303–2318.
23. Dickinson, M. H. & Lighton, J. R. B. (1995) *Science* **128,** 87–89.
24. Levine, J. & Hughes, M. (1973) *J. Morphol.* **140,** 153–158.
25. Miyawki, A., Griesbeck, O., Heim, R. & Tsien, R. Y. (1999) *Proc. Natl. Acad. Sci. USA* **96,** 2135–2140.